Influence of Mn doping on structural and optical properties of ZnO nano thin films synthesized by sol-gel technique

H. Merzouk[1], A. Chelouche[1], S. Saoudi[1], D. Djouadi[1], A. Aksas[1]

[1] Laboratoire du Génie de l'Environnement (LGE), Université de Béjaia, Algérie

*corresponding author, E-mail: hamid.merzouk@yahoo.fr

Abstract

Undoped and Mn-doped ZnO samples with different percentage of Mn content (1, 5 and 10 at l %) were synthesized by a dip-coating sol-gel method. We have studied the structural, chemical and optical properties of the samples by using X-ray diffraction (XRD), scanning electron microscopy (SEM), and UV–VIS spectroscopy. The XRD spectra show that all the samples are hexagonal wurtzite structures. We note that doping favors c-axis orientation along planes (002). Up to 5at% of Mn doping level, c-axis lattice parameter shifts towards higher value with the increase of manganese content in the films. The expansion of the lattice constant of ZnO-Mn indicates that Mn is really doped into the ZnO. The SEM investigations of all samples revealed that the crystallites are of nanometer size. The surface quality of the ZnO-Mn film increases with Mn doping but no significant changes of the grain size is observed from SEM images. The transmittance spectra show that the transparency of all the samples is greater than 85%. We note, also, that a small doping (1%) lowered the refractive index while the thickness of the layers and the gap increases. However, raising the proportion of Mn beyond 5%, practically the same values of index and gap than pure ZnO are found.

1. Introduction

Semiconductor nanostructures are of great interests for their well-known performance in electronics, optics and photonic. Zinc oxide, a member of II-VI group with a wide band gap (3.31 eV) and a large exitonic binding energy (60 meV) [1, 2], has been used in a wide range of device applications due to its semi-conducting, optical, electrical and piezoelectric properties [3]. ZnO is a good candidate as optoelectronic device material for use in the blue and violet regions. Good c-axis orientated crystalline structure is desirable for applications where crystallographic anisotropy is need such as piezoelectric surface acoustic wave devices. Diverse others properties such as optical transparency in the visible region, high voltage-current nonlinearity, chemical stability, biocompatibility, etc, impose ZnO material in different applications like short-wavelength light-emitting devices, transparent electrodes, gas sensor, solar cells[4].

The transition metal-doped ZnO has the potential to be multifunctional material with coexisting optical, semi-conducting and magnetic properties. The interest in doping ZnO is to explore the possibility of improving this characteristics .The doping of transition metal elements into ZnO allows the creation of sub energy levels in the band gap to make use as UV detector and light emitters. It has been reported that the band gap reduces for low concentration doping (3 at %), and increases for higher concentration [5, 6]. For the low-concentration Mn doping, the reduction in the band gap has been theoretically explained as a consequence of exchange interaction between d electrons of the transition metal ions (Mn) and the s and p electron of the host band. For the higher concentration (> 3 mol %) Mn doping, the augmentation is due to the large band gap of the MnO (4.2 eV) [7]. Recently, magnetic properties including room temperature ferromagnetism have been reported and can be applied to short-wave magneto-optical devices [8].
On the other hand, dilute magnetic semiconductors in which magnetic ions substitute cations of the host semiconductor material are assumed to be an ideal system for spintronics. Such materials have potential to revolutionize the electronic industries such as silicon-based volatile data storage processing and nonvolatile ferromagnetic recording media [9].

There are many reports in the literature about describing the preparation of ZnO thin films by a variety of techniques, including pulsed laser deposition, RF magnetron sputtering, chemical vapor deposition (CVD), molecular beam epitaxy (MBE), spray pyrolysis [11,14], etc. Sol-gel process is simple, inexpensive and has advantage of uniformity of deposit film thickness and, also, a large area deposition. Sol-gel thin film deposition is a good alternate to obtain particle size less than 20 nm and provides excellent control of composition.

So far, it has been much reported that ZnO were doped with In, Al, Ga, P, N, Li, and Mg for electrical and optical applications [17]. Some papers on ZnO films with Mn^{2+} doped concentrating for ferromagnetic properties have reported to [18]. However, ZnO films doped with Mn^{2+} applied for piezoelectric devices have not many reports. The goal of this work is to synthesis the Mn-doped samples using sol–gel dip- coating and to analyze the effect of doping on structural, surface morphology and optical properties of nano thin films.

2. Experimental

2.1. Synthesis

Mn doped ZnO thin films were obtained by sol-gel process. Zinc acetate, ethanol and diethanolamine are respectively used as precursor, solvent and stabilizer. Manganese acetate was used as source of doping. ZnO sol was obtaind by dissolving zinc acetate 0.6 M under stirring at 50 ° C in a solution of ethanol and DEA for 1 hour. Mn doped ZnO sol was done by adding zinc acetate and manganese acetate simultaneously to the solution of ethanol and DEA. A dip coater (KSV) apparatus was used for deposing thin layers on glass substrates with a withdrawal rate of 20 mm / min. After each deposition, the as-deposit films were dried at 150 ° C for 40 min. The operation was repeated until 3 layers. Then the samples obtained were calcined at temperature 550 ° C. Three sets of samples with different Mn doped level (1at%, 2at% and 3at %) were performed.

2.2. Characterizations

The thin films prepared were characterized by X-ray diffraction (XRD) at grazing incidence using the PanAnalytical diffractometer. X-rays are produced from a CuK radiation source (wavelength 1.54 Å), an acceleration voltage of 40 kV and a current of 30 mA. The SEM images were obtained by Zeiss scanning electron microscope. The optical transmittance spectra were obtained using a Jobin-Yvon HR460 UV-Visible.

2.3. Results and discussion

Figure.1 shows the XRD patterns of the undoped and doped ZnO: Mn films. All the peaks of the XRD patterns are indexed to ZnO with the hexagonal wurtzite structure. We note that doping favors orientation along planes (002). There is also reduction in the intensity of the peak (100) with increasing Mn concentration. Small peak broadening occurs with an increase of the manganese content. This indicates that the crystallite grain size increases with an increase of Mn percentage in the films (table1). The crystallite size D was calculated from the (0 0 2) peak width by using the Scherer's formula

$$D = \frac{0{,}89\lambda}{\Delta\theta\cos\theta} \qquad (1)$$

where D, λ, θ and β are the mean crystal size, the X-ray wavelength, Bragg diffraction angle and the FWHM of the (002) peak. D varies from 14.5 nm for 1at% Mn- doped samples to 17.1 nm for 5at% Mn-doped samples.

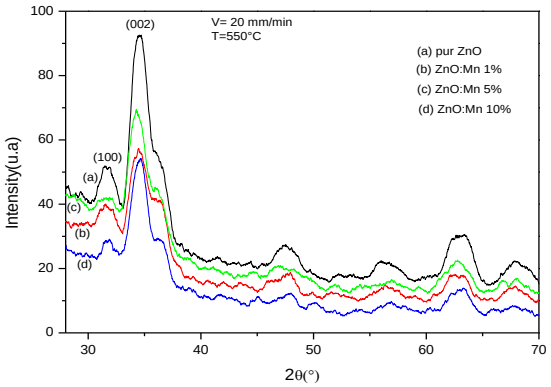

Fig. 1 X-ray diffraction spectra of the ZnO and ZnO: Mn films

Fig.2 shows the evolution of (002) peak spectra for different Mn concentration. The c-axis lattice is deduced using the relation [16]

$$c = \frac{\lambda}{sin\theta} \qquad (2)$$

The evolution of the c-axis lattice parameter is represented in table 2. Up to 5at% of Mn doping level, c-axis lattice parameter shifts towards higher value with the increase of manganese content in the films. This increase is due to the fact that ionic radius of Zn^{2+} (0.74A˚) is smaller than that of Mn^{2+} (0.83A˚). The expansion of the lattice constant of ZnO-Mn indicates that Mn is really doped into the ZnO. Above 5 at% Mn doping level, the linear increase of the c-axis with Mn concentrating is no longer respected as predicated by Viguard's law. This is most likely due to the small amount of precipitates that frequently arises during sol–gel growth.

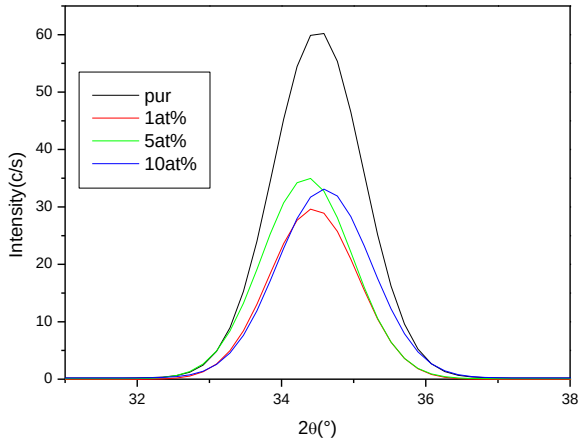

Fig.2 Evolution of the (002) peaks spectra with Mn doping level

Table 1: Average grain size of as-deposit films (002 peaks) for different concentrations

At% Mn-ZnO doping level	Grain size (nm)
0	18.2
1	14.5
5	17.1

Table 2: Lattice constants deduced from XRD data (002 peaks) of as-deposit films.

Lattice constants	ZnO	Mn-doped ZnO	
	0 at %	1 at %	5 at %
a (Å)	3.23	3.24	3.28
c (Å)	5.17	5.20	5.21

Fig.3 shows SEM images ZnO- Mn films. The SEM investigations of all samples revealed that the crystallites are of nanometer size. The surface quality of the ZnO-Mn film increases with Mn doping but no significant changes of the grain size is observed from SEM images.

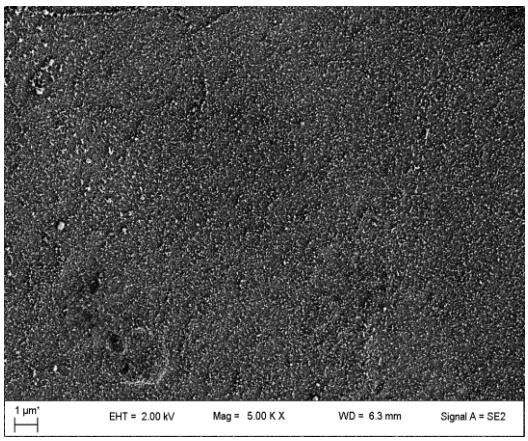

Fig.3: SEM micrograph of ZnO-Mn 5 at %

The optical transmittance spectra of pure ZnO and ZnO-Mn doped at 1 at%, 5% and 10 at% are shown in Figure 4. Between 340 and 450 nm the transmittance increases abruptly and then stabilized slightly above 80%. The increase of Mn concentration did not shift the edge of the transmittance. Only a low Mn doping (1%) significantly increases the transmittance between 400 and 500 nm. Elsewhere, the transmittance is almost unchanged. We note the presence of two minima around 520 nm.

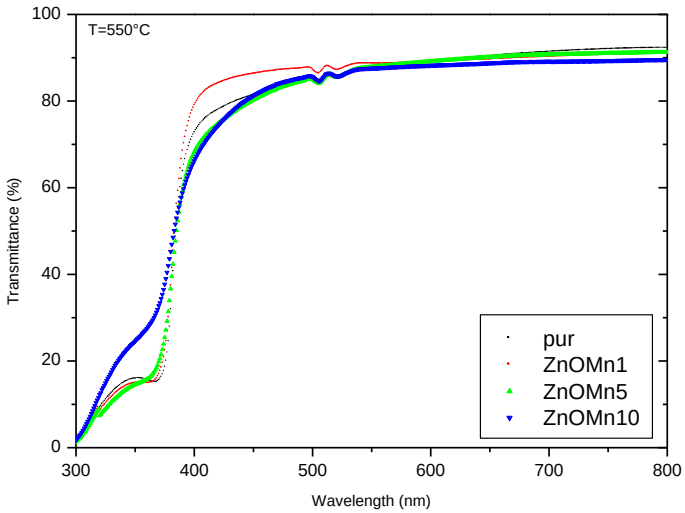

Fig.4: The transmittance spectra of ZnO and ZnO-Mn films

From these minima it is possible to calculate the refractive index using the relation [17]:

$$n = \sqrt{n_0 n_2}\left[\frac{1+\sqrt{1-T_{min}}}{\sqrt{T_{min}}}\right] \qquad (3)$$

where n_0 is the refractive index of air ($n_0 = 1$) and n_2 is the index of the substrate ($n_2 = 1.52$).
The thickness of the layers is calculated using the relation [16]:

$$\mathbf{d} = \frac{(2\mathbf{m}+1)\boldsymbol{\lambda}}{4\mathbf{n}} \qquad (4)$$

where m = 0, 1, 2, 3, is the order of T_{min} (m = 0 first concave curve) and n refractive index layer. We have summarized the results in Table 3:

Table 3: Refractive index, thickness and gap of as-deposit simples

Mn at %	refractive index	thickness (nm)	optical gap (eV)
0	1.89	267	3.22
1	1.80	280	3.23
5	1.88	269	3.21

We note that a small doping (1%) lowered the refractive index while the thickness of the layers and the gap increases. However, raising the proportion of Mn beyond 5%, practically the same values of index and gap than pure ZnO are found. Only the thickness of layers increases.

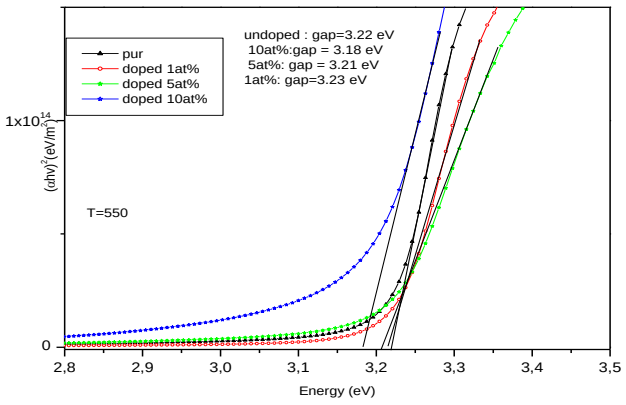

Fig.5 The plot of $(\alpha h\upsilon)^2$ vs. photon energy

4. Conclusion

The structural and optical properties of ZnO and ZnO-Mn films prepared by sol gel method were studied. The films exhibited the monocrystalline structure with hexagonal wurtzite. While the Mn incorporation deteriorated the crystalline structure of the ZnO film, the surface morphology of the ZnO film enhanced. We note that doping favors c-axis orientation along planes (002). Optical parameters were calculated and showed that the refractive index dispersion mechanism of both the ZnO and ZnO-Mn films obeys the single-oscillator model. The increase of Mn concentration did not shift the edge of the transmittance. Only a low Mn doping (1%) significantly increases the transmittance between 400 and 500 nm. Elsewhere, the transmittance is almost unchanged. Optical band gap energy measurements show the reduction in the band-gap just for 1at% Mn.

References

[1] Yu XB, Mao LH, Zhang F, Yang LZ, Yang SP (2004) Mater Lett 58:3661

[2] Viswanatha R,Sapra S,Gupta S, Satpati B, Satyam P V, Dev, Phys. Chem. B 108 (2004) 6303.

[3] Lee JB, Lee MH, Park CK, et al. Thin Solid Films 2004;447:296.Viswanatha R, Sapra S,Gupta S, Satpati B, Satyam P V,Dev, Phys. Chem. B 108 (2004) 6303.

[4] Chikoidze E, Dumont Y, von Bardeleben HJ, Gleize J, Jomard F,

[5] Venkataprasad S,Deepak F L. Solid State Commun 135 (2005) 345.

[6] Zhang XT, Liu YC, Zhang JY, et al. J Cryst Growth 2003; 254:80.
Rzepka E, Berrerar G, Ferrand D, Gorochov O (2007) Appl Phys
A 88:167
[7] Akyuz I, Kose S, Atay F, Bilgin V (2006) Semicond Sci Technol
21:1620
[8] Singh P, Kaushal A, Kaur D (2009) J Alloys Comp 471:11
[9] Yadav HK, Sreenivas K, Gupta V (2006) J Appl Phys 99:083507
[10] Wang J, Chen W, Wang M (2008) J Alloys Comp 449:44
[11] Deepa M, Bahadur N, Srivastava AK, Chaganti P, Sood KN
[12] T. Dietl, H. Ohno, F. Matsukura, J. Cibert, D. Ferrand, Science 287 (2000) 1019.
[13] J. Han, P.Q. Mantas, A.M.R. Senos, J. Eur. Ceram. Soc. 22 (2002) 49.
[14] S.S. Kim, J.H. Moon, B.T. Lee, O.S. Song, J.H. Je, J. Appl. Phys. 95 (2004) 454.